Increasing the resolution of laser rangefinders using low frequency pulses

Sikandar M. Zulqarnain Khan* and Giorgio Buttazzo

Scuola Superiore Sant'Anna,
Via Moruzzi, 1,
56124 Pisa, Italy
Email: s.khan@sssup.it
Email: g.buttazzo@sssup.it
*Corresponding author

Abstract: Laser rangefinders are used in several applications for measuring the distance of a target. Distance is computed by measuring the time of flight of a light pulse to hit the target and come back. The resolution of these devices is strictly related to the precision for measuring time intervals, limited by the oscillator clock frequency of the time-to-digital converter. This paper proposes a novel technique that allows achieving high resolution distance measurements with lower clock frequencies, enabling the development of low cost laser rangefinders. The idea is to increase precision by integrating multiple coarse measurements performed at slightly different clock frequencies, which are properly selected and integrated to produce a time measure with a higher resolution.

Keywords: laser ranging; pulsed time-of-flight; time-to-digital converter; interpolated resolution.

Biographical notes: Sikandar M. Zulqarnain Khan graduated from the University of Engineering and Technology, Pakistan in 2005 in Computer Engineering and received his MS in Electronics/Electrical Engineering in 2010 from the Hanyang University, South Korea. Later on, he joined COMSATs Institute of Information Technology (CIIT), Pakistan as a faculty member. In 2014, he joined the Instituto de Telecomunicaes of Aveiro, Portugal, as a researcher. Currently, he is pursuing his PhD at the ReTiS lab of the Scuola Superiore Sant'Anna, Pisa, Italy. He is the author of several conference research papers. His research interests include real-time embedded systems and wireless vehicular networks.

Giorgio Buttazzo is a Full Professor of Computer Engineering at the Scuola Superiore Sant'Anna of Pisa. He graduated in Electronic Engineering at the University of Pisa in 1985, received his MS in Computer Science at the University of Pennsylvania in 1987, and PhD in Computer Engineering at the Scuola Superiore Sant'Anna of Pisa in 1991. From 1987 to 1988, he worked on active perception and real-time control at the G.R.A.S.P. Laboratory of the University of Pennsylvania, Philadelphia. He has been Program Chair and General Chair of the major international conferences on real-time systems and Chair of the IEEE Technical Committee on Real-Time Systems. He is the Editor-in-Chief of *Real-Time Systems* and Associate Editor of the *IEEE Transactions on Industrial Informatics*. He has authored seven books on real-time systems and over 200 papers in the field of real-time systems, robotics, and neural networks.

1 Introduction

A laser rangefinder is a device that measures the distance of a target from itself. In particular, a laser rangefinder (Goldstein and Dalrymple, 1967) (also referred to as laser radar) estimates distance by transmitting a short laser pulse towards the target and measuring the time of flight (ToF) of the reflected pulse detected by an optical sensor. The distance to the target is then calculated by multiplying the ToF of the pulse with the known velocity of light (Nissinen et al., 2003). A laser radar, hence, consists of a laser transmitter, an optical detector, a time-to-digital converter

(TDC), and a microcontroller for the necessary computations. A block diagram illustrating such components is shown in Figure 1.

Precise distance measurement and real-time distance evaluation is required in several domains like robotics, navigation, camera auto-focusing, vehicular traffic monitoring, traffic congestion control, sports, mobile robot localisation, and military systems (Nissinen and Kostamovaara, 2009; Song et al., 2015; Pu et al., 2015). In surveillance systems, laser rangefinders could effectively be used in conjunction with vision systems for energy efficiency: a camera could be activated only when some

intrusion is detected based on distance measurements (Chen et al., 2014). Laser rangefinders have also been used for reconstructing real world scenarios in virtual reality applications (Dias et al., 2006; Amato et al., 2015). In industrial applications, laser radars are required for measuring the level of liquids in containers and profiling or scanning surfaces. In military systems, they are used for target identification and missile guidance, whereas in traffic safety applications they are used for obstacle detection, road edge recognition, position estimation, and collision avoidance (Kaisto et al., 1993; Kawashima et al., 1995; Määtta et al., 1993; Tanaka and Kochi, 2013; Wang et al., 2010).

Figure 1 Block diagram of a laser radar (see online version for colours)
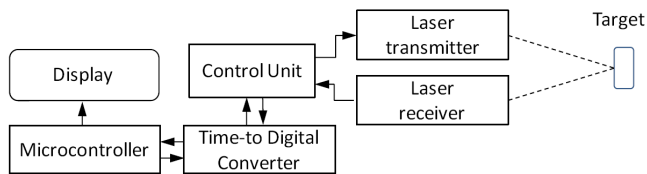
The measurement ranges and accuracy required by a laser radar greatly vary with the specific application in which it is used (Nissinen and Kostamovaara, 2009). For example, the measurement ranges vary from a few metres to some tens of metres in industrial applications and up to several kilometres in military applications. Similarly, the accuracy required by a laser radar also depends upon the specific application in which it is used. The precision required in industrial applications ranges from a few millimetres to some metres; whereas some military applications require precision ranging from tens to hundreds of metres (Nissinen and Kostamovaara, 2009).

The accuracy of pulsed laser rangefinder is determined by the time resolution of its TDC (Nissinen et al., 2003). In the simplest case, the TDC is just a counter that measures the time interval of any event by counting the number of clock pulses of an oscillator running at a given frequency. Hence, the resolution of such a counter-based TDC is limited by the minimum time period of the oscillator. For example, using a clock frequency of 100 MHz the time resolution is 10 ns corresponding to a spatial resolution of about 1.5 metres (Nissinen and Kostamovaara, 2009).

To achieve higher resolutions, several interpolation techniques have been proposed in the literature. For example, Kostamovaara and Myllylä (1986) described an analogue interpolation circuit composed of two time-to-amplitude converters for digitising the time fractions. This specific TDC combines the good single-shot accuracy of time-to-amplitude conversion with the long measurement range of the direct counting method. The effects of averaging the measurement results on the resolution and accuracy of the device are also discussed.

Määtta and Kostamovaara (1998) described another interpolation method that increases the resolution from 10 ns to 10 ps, while improving the stability by a real-time calibration procedure. Similarly, a time interval

measurement unit based on a counter and two-level interpolation with stabilised delay lines has been presented by Jansson et al. (2006). Such stabilised delay lines not only improve the nonlinearity of the interpolator but also enable the use of a lower clock frequency.

Raisanen-Ruotsalainen et al. (2000) exploited a counter-based TDC utilising two separate time digitisers interpolating within the clock period. These interpolators are based on analogue dual-slope conversion achieving a single-shot precision of 30 ps. Szplet et al. (2000) proposed another technique able to reduce the random error from 170 ps to 70 ps by a software correction of the nonlinearity of the delay lines.

A Vernier-based TDC has been discussed by Ronald (1970) and Rashidzadeh et al. (2010), where the achievable resolution is in the range of a few tens of picoseconds. A review of the time-interval measurements in the sub-nanosecond regime was presented by Porat (1973), who compared the various methods in terms of precision, stability, resolution, and other essential parameters. Calibration methods, stabilisation, and correction for time walk were also discussed.

All the techniques discussed above give excellent results exploiting high clock frequencies of the oscillator and complex digital circuitry, resulting in high-cost devices. However, in some industrial scenarios where targets are usually stationary, it would be beneficial to achieve high precision with low-cost and low-frequency oscillators.

1.1 Paper contribution

This paper proposes three measurement methods for pulsed laser radars to achieve higher resolutions with low oscillator frequencies at the cost of an increased measurement time. The spatial error and the extra number of measurements needed to achieve a desired resolution are carefully analysed and evaluated by a set of simulation experiments. The operation and performance of the proposed method is based on an off-chip re-configurable ring oscillator capable of generating multiple frequencies.

1.2 Paper organisation

The rest of this paper is organised as follows: Section 2 formally states the problem addressed in the paper. Section 3 proposes two techniques that can be used to reduce the error exploiting a reconfigurable ring oscillator. Section 4 presents an improved technique that allows reducing the number of measures with a more precise control of the resolution. Section 5 illustrates the algorithm for efficiently implementing the improved method. Section 6 presents some experimental results aimed at evaluating the proposed methods under different operating conditions. Finally, Section 7 states our conclusions.

2 Problem statement

Counter-based laser rangefinders compute the distance to a target by estimating the ToF of a light pulse to hit the target and come back. For a target located at distance d from the rangefinder, the ToF T_r is given by

$$T_r = \frac{2d}{c}.$$ (1)

where c is the speed of light ($c \simeq 3 \cdot 10^8$ m/s). Such a time is measured by counting the number N of periods of a reference clock elapsed from a start signal (synchronously generated with the light pulse) to a stop signal (produced when the reflected pulse is received by the optical sensor). If T_e is the ToF estimate measured by this method, the distance estimate d_e is computed by reversing equation (1), that is, as

$$d_e = \frac{cT_e}{2}.$$ (2)

Figure 2 If N is the counter value at the stop time t_r, the ToF T_r is always included in the interval $[NT_0, (N+1)T_0)$ (see online version for colours)
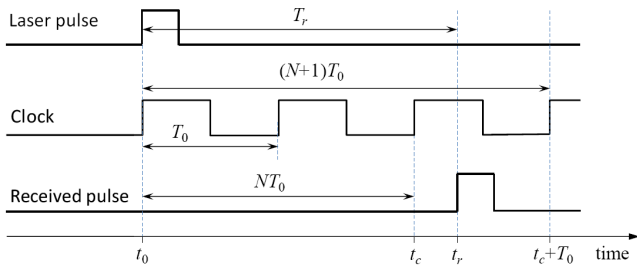
Hence, $\varepsilon_d = |d - d_e|$ represents the spatial error of the measure. Such an error is due to the fact that the arrival time of the reflected pulse is asynchronous with the edges of the clock used in the counter. To better explain the problem, consider the case shown in Figure 2, in which the reference clock frequency is f_0, giving a clock period $T_0 = 1 / f_0$. In this example, the reflected pulse generating the stop signal arrives at time t_r, within the third cycle of the clock, so the counter is stopped when its counter value is $N = 2$. In general, since the counter counts the number N of integer periods elapsed from the start time t_0 to the stop time t_r, the actual ToF interval $T_r = t_r - t_0$ is always included in the following range:

$$\frac{N}{f_0} \leq T_r < \frac{N+1}{f_0}.$$ (3)

Hence, the estimated ToF T_e can be computed as the average between the two extreme values of the interval:

$$T_e = \frac{2N+1}{2f_0}.$$ (4)

Clearly, the time resolution τ of this method is equal to the clock period T_0, while the timing error of a specific measure is given by the difference $\varepsilon_t = T_r - T_e$. Hence, the maximum timing error is given by $\varepsilon_t^{max} = T_e - NT_0 = (N+1)T_0 - T_e = T_0 / 2$.

Substituting equation (4) into equation (2), the distance can be estimated as follows:

$$d_e = (2N+1)\frac{c}{4f_0}.$$ (5)

Observe that the two limit values of the range for T_r provide two corresponding bounds for the actual distance d: a lower bound d_{lb} and an upper bound d_{ub}:

$$d_{lb} = N\frac{c}{2f_0}$$ (6)

and

$$d_{ub} = (N+1)\frac{c}{2f_0}.$$ (7)

Hence, the spatial resolution σ of this method is given by

$$\sigma = d_{ub} - d_{lb} = \frac{c}{2f_0},$$ (8)

whereas the maximum spatial error ε_d^{max} achievable in a distance measurement is given by

$$\varepsilon_d^{max} = \frac{d_{ub} - d_{lb}}{2} = \frac{\varepsilon_t^{max}c}{2} = \frac{c}{4f_0}.$$ (9)

Equation (8) allows deriving the minimum frequency f_0 needed to achieve a desired spatial resolution σ:

$$f_0 = \frac{c}{2\sigma}.$$ (10)

From equation (6), we can see that the minimum detectable distance d_{min} is the distance at which the counter counts at least one period ($N = 1$), that is

$$d_{min} = \frac{c}{2f_0}.$$ (11)

The maximum distance d_{max} is determined by the maximum number N_{max} that can be counted by the TDC, which depends on the number n of bits of the counter ($N_{max} = 2^n - 1$). That is,

$$d_{max} = N_{max}\frac{c}{2f_0}.$$ (12)

The major problem of the measuring method described above is that spatial resolutions in the order centimetres require clock frequencies in the order of GHz. For instance, equation (10) tells us that the minimum clock frequency for achieving a spatial resolution $\sigma = 1$ cm is $f_0 = 15$ GHz. As mentioned in Section 1, however, higher frequencies imply higher costs and higher energy consumption, which can be relevant issues in some specific applications. To overcome such a problem, the next section proposes two techniques

that can achieve the same resolution with lower clock frequencies.

3   Proposed approach

The spatial resolution obtained by a measure that uses a low clock frequency can be improved by performing additional measurements at slightly different frequencies, thus trading precision with measurement time. In particular, the following two alternative techniques are considered in this section:

- *F-inc*: This method performs multiple measures by slightly increasing the reference clock frequency, until the number of counts *increases* by one.

- *F-dec*: This method performs multiple measures by slightly decreasing the reference clock frequency, until the number of counts decreases by one.

For all the methods proposed in this paper, it is assumed that the target is stationary.

3.1   The F-inc method

The idea behind the F-inc method is to perform multiple measures at slightly increased frequencies $f(k)$ obtained by incrementing the previous one by a constant gap factor G:

$$f(k) = f_0 + kG, \qquad k = 0, 1, 2, \dots \qquad (13)$$

If N_0 is the number of counts obtained in the first measurement (for $k = 0$), the iteration process continues until a frequency f_m is found (for $k = m$) such that the number of counts becomes $N_0 + 1$ (note that m represents the number of steps performed in the iteration):

$$f_m = f(m) = f_0 + mG.$$

The iterative procedure is illustrated in Figure 3 for a case in which the counter value in the first measurement is $N_0 = 1$ and becomes 2 after $m = 5$ iterations. Then, the ToF is estimated as the average between $(N_0 + 1)T_m$ and $(N_0 + 1)T_{m-1}$, that is

$$T_e = (N_0 + 1) \frac{2f_m - G}{2f_m(f_m - G)}, \qquad (14)$$

whereas the distance is computed according to equation (2), as $d_e = T_e c / 2$.

The time resolution τ^+ that can be obtained with this approach is given by the following Lemma.

Lemma 1: If N_0 is the number of counts got in the first measurement, the time resolution τ^+ achieved with the F-inc method, using a frequency gap G, is given by

$$\tau^+ = \frac{(N_0 + 1)G}{f_0(f_0 + G)}. \qquad (15)$$

The time resolution can be computed by assuming the worst-case situation in which, at step $m - 1$, the rising edge arrives just after the stop signal, as illustrated in Figure 4, where for convenience only the clock rising edges are shown.

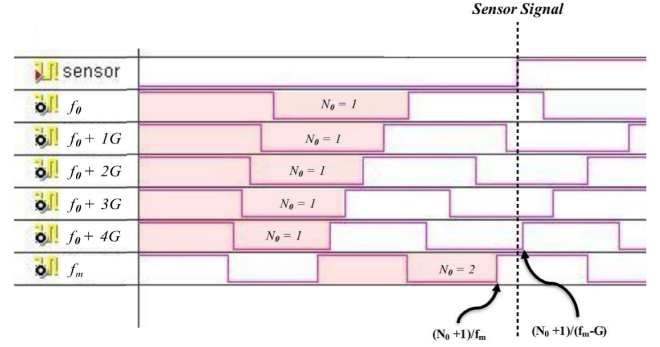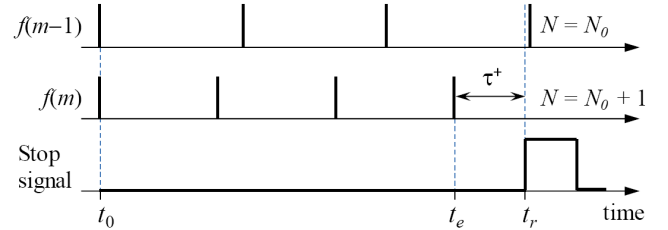Figure 3   Example of iterative measurements with the F-inc method (see online version for colours)

Figure 4   Time resolution τ^+ achievable by F-inc (see online version for colours)

In this situation, in fact, at step m, the rising edge moves to the left (at time t_e) by the largest amount. Hence, it results that

$$\tau^+ = t_r - t_e = \frac{N_0 + 1}{f(m-1)} - \frac{N_0 + 1}{f(m)} = \frac{(N_0 + 1)G}{f(m-1)f(m)}$$

and from equation (13), we get:

$$\tau^+ = \frac{(N_0 + 1)G}{(f_0 + mG - G)(f_0 + mG)}.$$

We now observe that τ^+ decreases with the value of m, as also shown in Figure 5, hence, the largest value for τ^+ occurs for the minimum value of m, that is, after the first increment ($m = 1$). Thus, the lemma follows. ☐

Figure 6 reports the aforementioned phenomenon in a graphical way showing how the time resolution τ^+ varies as a function of the reference frequency f_0 for different values N_0 of the counter (in this graph G is equal to 10 MHz).

The maximum number of steps M required by F-inc can be found considering the worst-case situation in which in the first measurement at frequency f_0 the stop signal arrives just after the N_0^{th} raising front, as depicted in Figure 7. In this case, the frequency f_M causing the counter increment is such that

$$\frac{N_0 + 1}{f_M} = \frac{N_0}{f_0}$$

that is

$$f_M = \frac{N_0 + 1}{N_0} f_0$$

and since $f_M = f_0 + MG$, it results that

$$M = \left\lceil \frac{f_0}{N_0 G} \right\rceil. \tag{16}$$

Note that, the value of M depends on the target distance (through the counter value N_0), thus in the worst case the maximum number of steps performed by the F-inc method will occur for the minimum counter value ($N_0 = 1$) and is given by

$$M = \left\lceil \frac{f_0}{G} \right\rceil. \tag{17}$$

Figure 5 The time resolution τ^+ decreases as the frequency increases (see online version for colours)
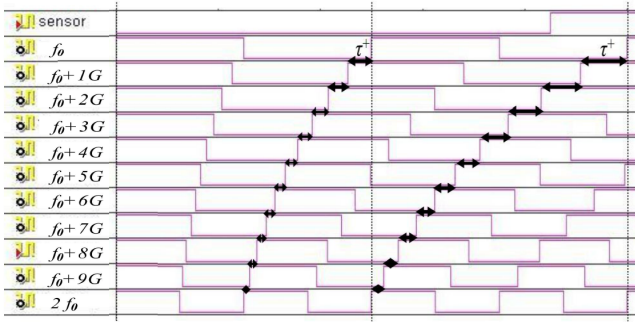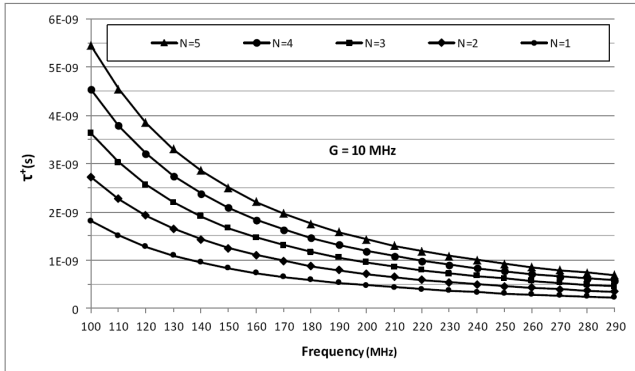
Figure 6 Maximum timing error ε^+ as a function of the frequency for different counter values
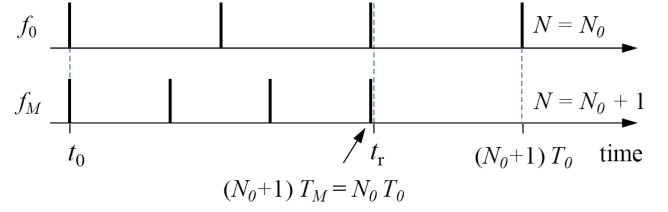
3.2 The F-dec method

The F-dec method is similar to F-inc, with the difference that the various measures are performed using decreasing frequencies $f(k)$ obtained by decrementing the previous one by a constant gap factor G:

$$f(k) = f_0 - kG, \qquad k = 0, 1, 2, \ldots \tag{18}$$

Figure 7 Worst-case scenario determining the maximum number of steps for the F-inc method (see online version for colours)

If N_0 is number of counts obtained in the first measurement (for $k = 0$), the iteration process continues until a frequency f_m is found (for $k = m$) such that the number of counts becomes $N_0 - 1$ (note that m represents the number of steps performed in the iteration):

$$f_m = f(m) = f_0 - mG.$$

The time resolution τ^- that can be obtained with this approach is given by the following lemma.

Lemma 2: If N_0 is the number of counts got in the first measurement, the time resolution τ^- achieved with the F-dec method, using a frequency gap G, is given by

$$\tau^- = \frac{(N_0 + 1)^2 G}{f_0 (f_0 N_0 - G N_0 - G)}. \tag{19}$$

The largest timing error can be computed by assuming the worst-case situation in which that, at step $m - 1$, the rising edge arrives just before the stop signal, as illustrated in Figure 8. In this situation, in fact, at step m the rising edge moves to the right (at time t_e) by the largest amount.

Figure 8 Timing resolution τ^- achievable by F-dec (see online version for colours)
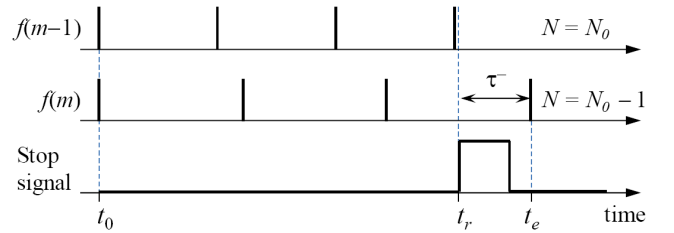
From the situation depicted in Figure 8, it results that

$$\tau^- = t_e - t_r = \frac{N_0}{f(m)} - \frac{N_0}{f(m-1)} = \frac{N_0 G}{f(m) f(m-1)}$$

and from equation (18), we get:

$$\tau^- = \frac{N_0 G}{(f_0 - mG)(f_0 - mG + G)}. \tag{20}$$

We now observe that τ^- increases with the value of m, so the worst-case error can be derived by assuming the maximum value for m. The largest value of m (compatible with the value N_0 counted on the first measurement) is given by the case illustrated in Figure 9, in which the clock rising edge located just before the stop signal, at frequency f_0, is shifted by exactly one period $1 / f_0$ in $m - 1$ steps, thus moving from

time $t_p = N_0 / f_0$ to time t_r, almost equal to $(N_0 + 1) / f_0$. Hence, the highest value of m can be found by imposing that
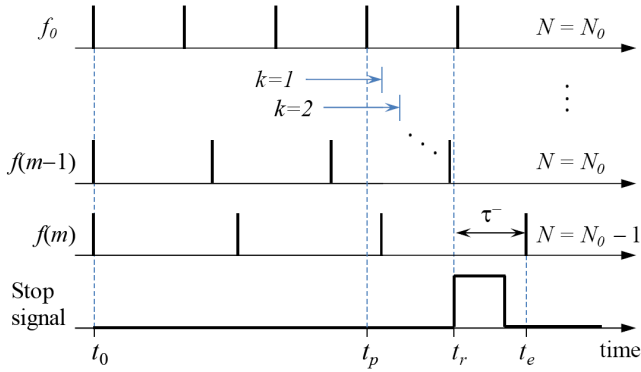
$$\frac{N_0}{f(m-1)} = \frac{N_0}{f_0} + \frac{1}{f_0} = \frac{N_0+1}{f_0},$$

and from equation (18) we get:

$$mG = G + \frac{f_{10}}{N_0+1}.$$

Substituting this value of mG in equation (20) the lemma follows.   ☐

Figure 9   Worst-case situation considered in Lemma 2 (see online version for colours)

The maximum number of steps M required by F-dec can be found considering the worst-case situation in which in the first measurement at frequency f_0 the stop signal arrives just before the $(N_0 + 1)^{th}$ raising front, as depicted in Figure 10. In this case, the frequency f_M causing the counter decrement is such that
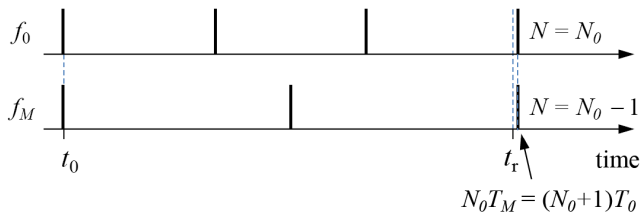
$$\frac{N_0}{f_M} = \frac{N_0+1}{f_0}$$

that is

$$f_M = \frac{N_0}{N_0+1}f_0$$

and since $f_M = f_0 - MG$, it results that

$$M = \left\lceil \frac{f_0}{(N_0+1)G} \right\rceil. \qquad (21)$$

Figure 10   Worst-case scenario determining the maximum number of steps for the F-dec method (see online version for colours)

3.3   Comparison

Using the results of Lemma 1 and Lemma 2, the following theorem proves that the maximum timing error achieved by F-inc is always smaller than that achieved by F-dec.

Theorem 3: For any reference clock frequency f_0 and gap value G, the worst-case error achieved by F-inc is always smaller than the worst-case error achieved by F-dec.

Taking the ratio of the resolutions derived in Lemma 1 and Lemma 2, we have:

$$\frac{\tau^+}{\tau^-} = \frac{f_0 \dfrac{N_0}{N_0+1} - G}{f_0 + G}. \qquad (22)$$

Being $\dfrac{N_0}{N_0+1} < 1$ for any integer count N_0, we can write

$$\frac{\tau^+}{\tau^-} = \frac{f_0 \dfrac{N_0}{N_0+1} - G}{f_0 + G} < \frac{f_0 - G}{f_0 + G} < \frac{f_0 + G}{f_0 + G} = 1.$$

Thus, the theorem follows.   ☐

Since F-inc is better than F-dec, the rest of this section illustrates how to determine the frequency gap G for achieving a desired spatial resolution σ and how to estimate the maximum number of steps.

It is worth observing that while the time resolution of a single-shot measure is only a function of the clock frequency ($\tau = 1 / f_0$), the time resolution τ^+ achieved by the F-inc method, expressed by equation (15), depends on both N_0 (i.e., the target distance) and the gap factor G. In particular, if both methods use the same clock frequency f_0, the F-inc method improves the single-shot measure if

$$\frac{(N_0+1)G}{f_0(f_0+G)} < \frac{1}{f_0}$$

that is, if

$$G < \frac{f_0}{N_0}. \qquad (23)$$

Since N_0 depends on the distance, to guarantee a resolution improvement for any possible target distance, equation (23) must hold for any value of N_0, and in particular for the value N_{max} corresponding to the maximum distance d_{max}. The value N_{max} can be derived from equation (12) and is given by

$$N_{max} = \frac{2f_0}{c} d_{max}. \qquad (24)$$

Substituting equation (24) into equation (23) we get

$$G < \frac{c}{2d_{max}}. \qquad (25)$$

Equation (25) imposes a condition on the maximum gap factor G_{max} for guaranteeing a resolution improvement by

the F-inc method with respect to the single-shot measurement, so we can write

$$G_{max} = \frac{c}{2d_{max}}.$$ (26)

4 Improved method

This section presents an improved method which allows reducing the number of steps and achieving a constant timing error ε independent of the step value.

Let f_0 be the reference frequency used in the first measure and let N_0 be the corresponding value of the clock counter. From the example illustrated in Figure 11, it is easy to see that in the worst case in which the stop signal arrives at time t_r, just after N_0 clock periods T_0, the maximum clock frequency f_m that has to be generated to achieve an increment of the clock counter is such that $(N_0 + 1)T_m = N_0 T_0$, that is:

$$f_m = \frac{N_0 + 1}{N_0} f_0.$$ (27)

Figure 11 Increasing the frequency to achieve a constant error τ (see online version for colours)
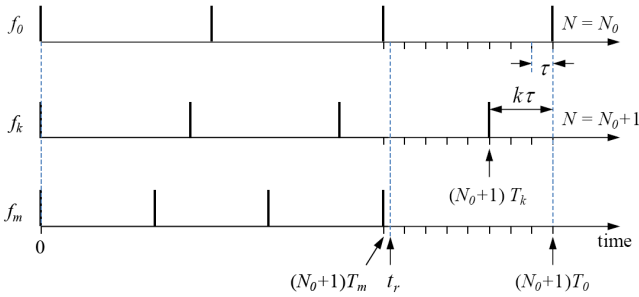
The idea behind the improved method is to divide the time interval $[N_0 T_0, (N_0 + 1)T_0]$ into an integer number of m equal subintervals of size τ equal to the desired time resolution so that, at any step k, the $(N_0 + 1)^{th}$ clock rising edge at frequency f_k reduces exactly by τ with respect to the previous step. This means that, after k steps from the initial measure, the $(N_0 + 1)^{th}$ rising edge of the clock at frequency f_k is located at time

$$(N_0 + 1)T_k = (N_0 + 1)T_0 - k\tau.$$

Hence, the clock period at step k is

$$T_k = T_0 - \frac{k\tau}{N_0 + 1}$$ (28)

and the clock frequency at step k is

$$f_k = \frac{f_0}{1 - \left(\frac{k\tau}{N_0 + 1}\right)f_0}.$$ (29)

Note that for $k = 0$, equation (29) gives $f_k = f_0$, and for $k = m$ (being $m\tau = T_0 = 1 / f_0$) it gives the expression for f_m found in equation (27).

If the measuring refining policy starts from the reference frequency f_0 and generates the subsequent frequencies by increasing k one by one, it is clear that the maximum number M of measures needed to find the counter increment from N_0 to $N_0 + 1$ is exactly m (as shown in the example illustrated in Figure 11).

By using a bisection method, however, the maximum number of steps can be significantly reduced and becomes

$$M = \lceil \log_2 m \rceil.$$ (30)

In this case, if the interval T_0 is divided in a number of subintervals equal to a power of 2, (e.g., $m = 2^a$), then the maximum number of measures needed to find the counter increment is $M = a$.

Considering that the spatial resolution σ is related to the time resolution τ by the following relation [see also equation (9)[

$$\sigma = \tau \frac{c}{2},$$

then, the number m of intervals into which T_0 has to be divided can be expressed as a function of the desired spatial resolution σ:

$$m = \left\lceil \frac{T_0}{\tau} \right\rceil = \left\lceil \frac{c}{2f_0 \sigma} \right\rceil.$$ (31)

Substituting equation (31) into equation (30), it results that the maximum number of steps needed to perform the measurement with a resolution σ is

$$M = \left\lceil \log_2 \left\lceil \frac{c}{2f_0 \sigma} \right\rceil \right\rceil.$$ (32)

To appreciate the advantage of the bisection method, suppose that a spatial resolution $\sigma = 10$ cm is required for a given application. According to equation (10), the clock frequency required to achieve this resolution with a single-shot measure is

$$f_0 = \frac{c}{2\sigma} = \frac{3 \cdot 10^8}{2 \cdot 10^{-1}} = 1.5 \text{ GHz}.$$

Applying the F-inc method, the same resolution can be achieved with a reference clock frequency $f_0 = 100$ MHz, and a maximum gap factor $G = 1.5$ MHz, computed by equation (26), but up to 67 measurements may be needed, as stated by equation (17). Using the bisection method, however, equation (32) tells us that a spacial resolution of $\sigma = 10$ cm can be achieved with same frequency with a maximum number of measures equal to $M = \lceil \log_2 15 \rceil = 4$.

It is worth mentioning that while the resolution in the F-inc and F-dec methods depends upon the target distance (through N_0 and G), the improved bisection-based method is independent of the target distance. In this method, the resolution is an input parameter specified by the user that affects the number of measuring steps (M), as clear from equation (32).

The algorithm for implementing the bisection method is presented in the next section.

5   Algorithm

This section describes the algorithm for carrying out the measures according to the bisection method. Since now the frequency does not monotonically increase with the step index k, let $s_0, s_1, \ldots, s_M$ be the sequence of M steps performed by the algorithm, and let $f(s_0), f(s_1), \ldots, f(s_M)$ be the corresponding frequencies selected at each step. At step s_0, the first measure is always performed at the reference frequency $f(s_0) = f_0$, storing the number of clock counts in the variable N_0. At step s_1, the measure is always performed at a frequency $f(s_1) = f_k$ such that $k = m / 2$, so dividing the search interval in two equal parts:

$$f(s_1) = \frac{f_0}{1 - \frac{m\tau}{2(N_0 + 1)} f_0},$$

If with the frequency $f(s_1)$ the clock counter is still N_0, then the next frequency $f(s_2)$ has to be increased at the value $k = m / 2 + m / 4$, otherwise it has to be decreased at the value $k = m / 2 - m / 4$.

In general, if b denotes the size of the next time increment (measured in τ units), such a value must be divided by two at each step, while the index k of the frequency to be used at the next step can be computed as $k = k + b$, if the clock counter N of the current measure is found to be N_0, and as $k = k - b$, otherwise. By defining an auxiliary variable s that takes the value 1, if N is equal to N_0, and –1 otherwise, the next step can be computed as $k = k + s * b$.

Note that after the last measure $f(s_M)$, two cases can occur, as illustrated in Figure 12. In the first case, denoted as case (a), the stop signal arrives at time t_r, just before the $(N_0 + 1)^{th}$ raising front of the clock at frequency $f(s_M)$; hence, t_r is within the interval $[(N_0 + 1)T_k - \tau, (N_0 + 1)T_k]$, so that the estimated ToF can be computed as

$$T_e = \frac{N_0 + 1}{f_k} - \frac{\tau}{2}.$$

In the second case, denoted as case (b), the stop signal arrives at time t_r, just after the $(N_0 + 1)^{th}$ raising front of the clock at frequency $f(s_M)$; hence, t_r is located within the interval $[(N_0 + 1)T_k, (N_0 + 1)T_k + \tau]$, so that the estimated ToF can be computed as

$$T_e = \frac{N_0 + 1}{f_k} + \frac{\tau}{2}.$$

Now, noting that in case (a) $s = -1$ and in case (b) $s = 1$, the estimated ToF can be computed in both cases as

$$T_e = \frac{N_0 + 1}{f_k} + s\frac{\tau}{2}. \tag{33}$$

Figure 12   After the last measurement, the stop signal is found (a) before the $(N_0 + 1)^{th}$ front if $N = N_0$, and (b) after if $N = N_0 + 1$ (see online version for colours)
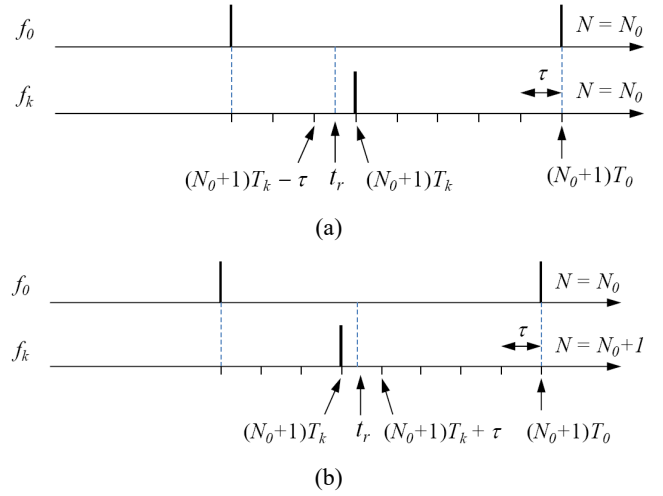
The algorithm that implements the sequence of measures using the bisection method is shown in Figure 13.

Figure 13   Pseudocode of the algorithm exploiting the bisection method

```
refined_measure(f0, σ) {

    m = ⌈ c / (2 f0 σ) ⌉;

    b = m;          // search interval
    k = 0;          // frequency index
    s = 1;          // sign flag

    N0 = measure(fk);

    while (b > 1) {

        b = b/2;
        k = k + s * b;
        N = measure(fk);

        if (N == N0) s = 1;
        else s = -1;
    }

    τ = 2σ/c;               // time resolution
    Te = (N0+1)/fk + s τ/2; // ToF estimate
    d = c * Te/2;           // distance estimate
    return (d);

}
```

The algorithm takes as input the reference clock frequency f_0 and the desired spatial resolution σ and returns the estimated distance to the target. The algorithm keeps track of the search interval through the variable b, which encodes the interval size in number of units (one unit is equal to the time resolution τ). The frequency f_k is computed as a function of the index k according to equation (29), where k varies from 0 to m. Then, a sign flag s is used to

discriminate between case (a) ($s = -1$) and case (b) ($s = 1$). At the beginning, b is initialised to the value of m given by equation (31) (corresponding to the full interval $T_0 = m\tau$), k is initialised to 0 (that is f_0), and s to 1. Note that within the while loop the interval is divided by 2 at each step, so the loop ends when $b \leq 1$, performing at most $\lceil \log_2 m \rceil$ iterations. Then the algorithm estimates the ToF according to equation (33) and finally computes the distance d according to equation (2).

6 Experimental results

This section reports a set of experiments aimed at evaluating the performance of the proposed measurement methods. All the results shown in the graphs are obtained by simulation using the following procedure:

1 For a given target distance d, the stop delay interval T_r is computed by equation (1) as $T_r = 2d / c$.

2 For a given reference clock frequency f_0, the counter value is then computed as $N_0 = \lfloor T_r f_0 \rfloor$.

3 Depending on the specific tested method (F-inc or bisection), a sequence of measuring steps is performed at different clock frequencies and, for each frequency f, the counter value is computed as $N = \lfloor T_r f \rfloor$, until the number of counts increases by one with respect to N_0. The number m of measuring steps and the final frequency f_m are stored in two corresponding variables.

4 The estimated ToF T_e is computed by equation (14) for the F-inc method and by equation (33) for the bisection method.

5 Finally, the target distance is estimated by equation (14) as $d_e = T_e c / 2$.

To have a reference to compare with, Figure 14 shows the spatial error achievable with a single-shot measure as a function of the clock frequency, for a target located at 20 m. Note that the actual error can potentially varies from 0 (in the best case in which the target is at a distance such that the ToF is multiple of T_0) to the maximum timing error ε_{max} given by equation (9). Note that in a single-shot measure, the maximum error ε_{max} is not affected by the target distance, but only depends on the clock frequency.

A second experiment was carried out to evaluate how the spatial error ε_d of the F-inc method varies as a function of the gap factor G. This test was performed for three different clock frequencies (50 MHz, 100 MHz, and 200 MHz) and the maximum target distance was set at $d_{max} = 20$ m. The results are reported in Figure 15. Note that, under this setting, the maximum gap factor that guarantees a resolution improvement of the F-inc method with respect to a single-shot measure is equal to $G_{max} = 7.5$ MHz, according to equation (25).

Since the error in the F-inc method also depends on the target distance, another test was performed to measure the spatial error $\varepsilon_d = |d - d_e|$ as a function of the distance, for different gap factors (1 MHz, 3 MHz, 5 MHz, and 7 MHz), fixing the clock frequency at 100 MHz. The result of this test is reported in Figure 16.

Figure 14 Spatial error achievable with a single measure as a function of the clock frequency
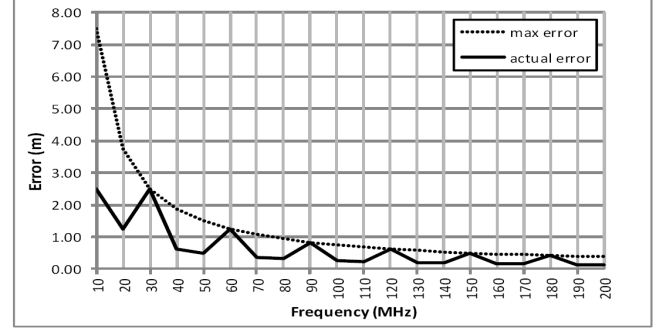

Figure 15 Spatial error of the F-inc method as a function of the frequency gap G, for different reference clock frequencies (see online version for colours)
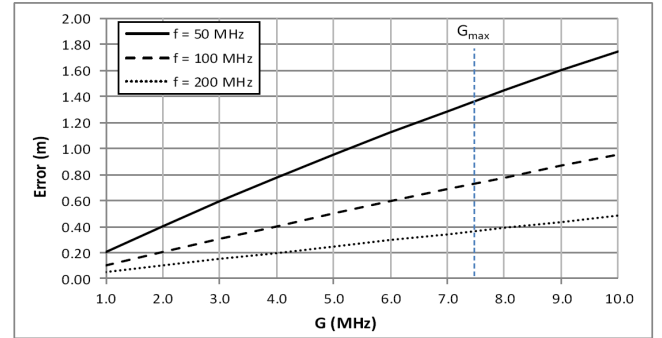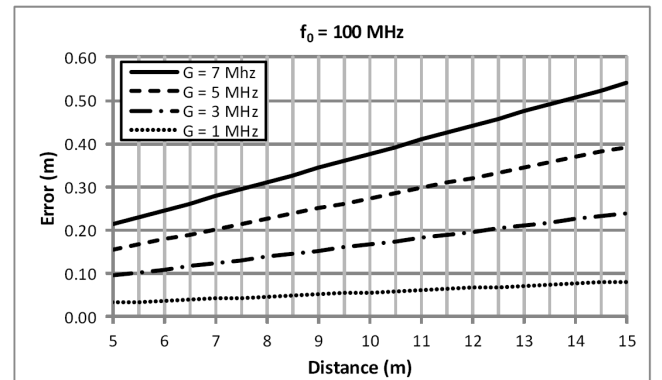

Figure 16 Spatial error of the F-inc method as a function of the target distance, for different gap values

A third experiment was performed to see how the gap factor and the number of steps are affected by the clock frequency in the F-inc method, for different resolutions. In particular, Figure 17 shows how the gap factor G should be set at a given clock frequency to achieve a desired resolution σ, whereas Figure 18 shows the corresponding number of steps required by F-inc for specific (f_0, σ) values.

A fourth experiment was performed to monitor the number of steps required by the F-inc and the bisection method as a function of the clock frequency. Figure 19 plots the results obtained by setting a resolution $\sigma = 1$ cm. Note that the F-inc method becomes impractical for clock frequencies lower than 750 MHz, requiring too many measuring steps, whereas the bisection method is still very effective at frequency of 50 MHz, requiring only nine steps.

Figure 17   Gap factor as a function of f_0 to achieve a desired resolution σ under F-inc
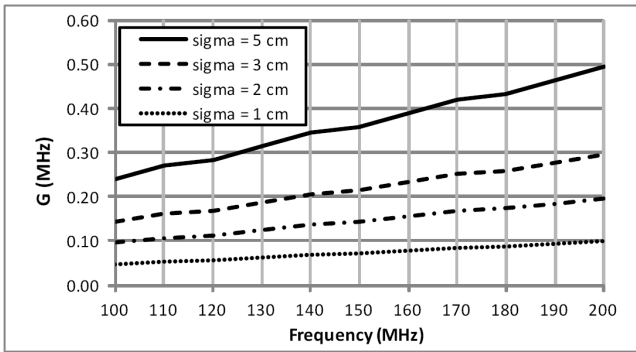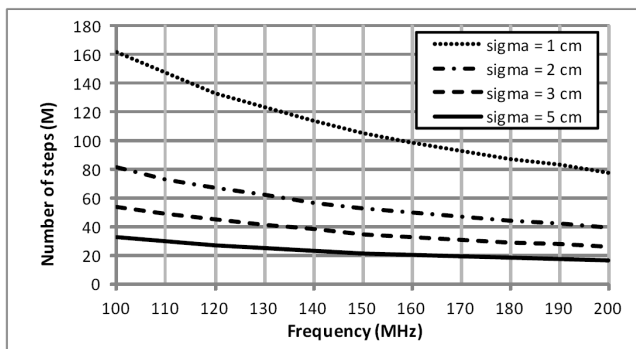

Figure 18   Number of steps required by F-inc as a function of f_0 for different resolutions

Considering the effectiveness of the improved algorithm, Figure 20 shows the number of steps achieved by the bisection method on a larger scale factor for different resolutions.

Figure 19   Number of steps achieved by the F-inc and bisection methods as a function of the clock frequency
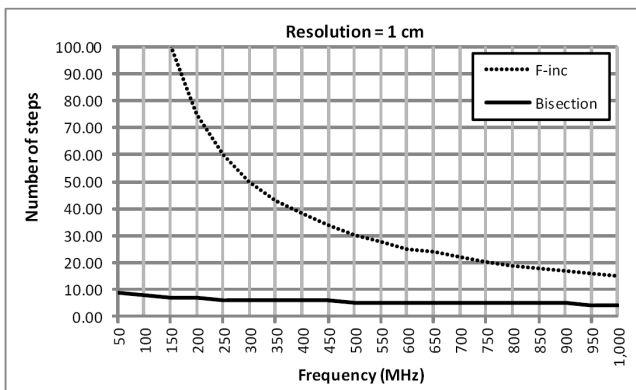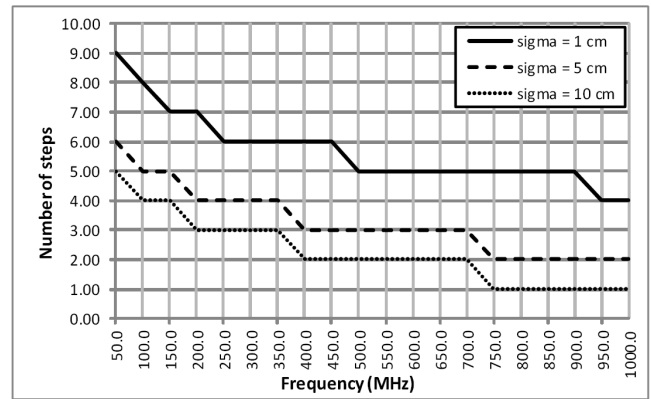

Figure 20   Number of steps achieved by the bisection method as a function of the clock frequency.

7   Conclusions

This paper presented three distance measurement methods for counter-based laser rangefinders that allow achieving high-resolution measurements by using relatively low-frequency reference clocks. In all the three approaches, the resolution is improved at the cost of an increased measurement time by iteratively performing a sequence of coarse measurements at slightly difference frequencies, where each frequency is selected as a function of the previous measure. In the first two methods (denoted as F-inc and F-dec), the reference frequency is monotonically increased or decreased by a constant gap factor, until the number of counts increases or decreases by one.

Although these two approaches are simpler to implement, they exhibit the following problems:

- The spatial error is not constant, but varies with the progress of measures; in particular, it decreases under F-inc and increases under F-dec.

- For a given spatial resolution σ, the number of measures is not constant, but varies from 1 up to a maximum number M, given by equation (17), depending on the specific target distance.

- To achieve spatial resolutions in the order of centimetres with a clock frequency no higher than 100 MHz, the number of measures becomes too high (greater than 100), since M is a hyperbolic function of σ.

To overcome these problems, the third method proposed in this work exploits a binary search procedure to quickly estimate the distance to the target in a reasonably low number of steps. In this approach, the clock frequency is not varied monotonically with the steps, but it is properly selected based on the previous measure. As a result, the number of steps required to achieve a desired spatial resolution σ does not depend on the target distance and is equal to the value provided by equation (32).

Finally, it should be mentioned that while a single-shot measurement takes a fraction of a microsecond (e.g., approximately 0.1 μs for a target at a distance of 15 m), the

measuring time required by the proposed bisection method is still in the range of microseconds, considering that the same resolution is achieved by fewer steps, which is quite below the human perception sensitivity.

In conclusion, the proposed methods, in particular the one based on bisection, enables the development of laser rangefinders using low-frequency components, thus reducing the cost without sacrificing the spatial resolution.

References

Amato, F., Mazzeo, A., Moscato, V., Picariello, A. and Sansone, C. (2015) 'Managing 3d objects for real world scenes reconstruction', *International Journal of Computational Science and Engineering*, Vol. 11, No. 1, pp.56–67.

Chen, C-P., Chuang, C-L., Lin, T-S., Liu, C-Y., Jiang, J-A., Yuan, H-W., Chiou, C-R. and Hong, C-H. (2014) 'Terncam: an automated energy-efficient visual surveillance system', *International Journal of Computational Science and Engineering*, Vol. 9, Nos. 1–2, pp.44–54.

Dias, P., Matos, M. and Santos, V. (2006) '3d reconstruction of real world scenes using a low-cost 3d range scanner', *Computer-Aided Civil and Infrastructure Engineering*, Vol. 21, No. 7, pp.486–497.

Goldstein, B.S. and Dalrymple, G.F. (1967) 'Gallium arsenide injection laser radar', *Proceedings of the IEEE*, Vol. 55, No. 2, pp.181–188.

Jansson, J-P., Mantyniemi, A. and Kostamovaara, J. (2006) 'A CMOS time-to-digital converter with better than 10 ps single-shot precision', *IEEE Journal of Solid-State Circuits*, Vol. 41, No. 6, pp.1286–1296.

Kaisto, I.P., Kostamovaara, J.T., Manninen, M. and Myllylae, R.A. (1993) 'Laser radar-based measuring systems for large scale assembly applications', in *Laser Dimensional Metrology: Recent Advances for Industrial Application*, pp.121–131, International Society for Optics and Photonics.

Kawashima, S., Watanabe, K. and Kobayashi, K. (1995) 'Traffic condition monitoring by laser radar for advanced safety driving', in *Proceedings of the Intelligent Vehicles' 95 Symposium*, IEEE, pp.299–303.

Kostamovaara, J. and Myllylä, R. (1986) 'Time-to-digital converter with an analog interpolation circuit', *Review of Scientific Instruments*, Vol. 57, No. 11, pp.2880–2885.

Määtta, K. and Kostamovaara, J. (1998) 'A high precision time-to-digital converter for pulsed time-of-flight laser radar applications', *IEEE Transactions on Instrumentation and Measurement*, Vol. 47, No. 2, pp.521–536.

Määtta, K., Kostamovaara, J. and Myllylä, R. (1993) 'Profiling of hot surfaces by pulsed time-of-flight laser range finder techniques', *Applied Optics*, Vol. 32, No. 27, pp.5334–5347.

Nissinen, I. and Kostamovaara, J. (2009) 'On chip voltage reference-based time-to-digital converter for pulsed time-of-flight laser radar measurements', *IEEE Transactions on Instrumentation and Measurement*, Vol. 58, No. 6, pp.1938–1948.

Nissinen, I., Mantyniemi, A. and Kostamovaara, J. (2003) 'A CMOS time-to-digital converter based on a ring oscillator for a laser radar', in *Solid-State Circuits Conference, 2003, ESSCIRC'03, Proceedings of the 29th European*, IEEE, pp.469–472.

Porat, D.I. (1973) 'Review of sub-nanosecond time-interval measurements', *IEEE Transactions on Nuclear Science*, Vol. 20, No. 5, pp.36–51.

Pu, L., Xu, X., He, H., Zhou, H., Qiu, Z. and Hu, Y. (2015) 'A flexible control study of variable speed limit in connected vehicle systems', *International Journal of Embedded Systems*, Vol. 7, No. 2, pp.180–188.

Raisanen-Ruotsalainen, E., Rahkonen, T. and Kostamovaara, J. (2000) 'An integrated time-to-digital converter with 30-ps single-shot precision', *IEEE Journal of Solid-State Circuits*, Vol. 35, No. 10, pp.1507–1510.

Rashidzadeh, R., Ahmadi, M. and Miller, W.C. (2010) 'An all-digital self-calibration method for a Vernier-based time-to-digital converter', *IEEE Transactions on Instrumentation and Measurement*, Vol. 59, No. 2, pp.463–469.

Ronald, N. (1970) *Digital Time Intervalometer with Analogue Vernier Timing*, 17 November, US Patent 3,541,448.

Song, H., Chen, Y. and Gao, Y. (2015) 'Real-time visibility distance evaluation based on monocular and dark channel prior', *International Journal of Computational Science and Engineering*, Vol. 10, No. 4, pp.375–386.

Szplet, R., Kalisz, J. and Szymanowski, R. (2000) 'Interpolating time counter with 100 ps resolution on a single FPGA device', *IEEE Transactions on Instrumentation and Measurement*, Vol. 49, No. 4, pp.879–883.

Tanaka, M. and Kochi, K. (2013) 'Initial position estimation of a mobile robot with a laser range finder by differential evolution', *International Journal of Advanced Mechatronic Systems*, Vol. 5, No. 6, pp.373–382.

Wang, H., Hu, Z. and Yu, H. (2010) 'Road edge recognition for mobile robot using laser range finder', *International Journal of Advanced Mechatronic Systems*, Vol. 2, No. 4, pp.236–245.